

See discussions, stats, and author profiles for this publication at: <https://www.researchgate.net/publication/6419932>

Atmospheric Chemistry of Linear Perfluorinated Aldehydes: Dissociation Kinetics of $C_n F_{2n+1}CO$ Radicals

ARTICLE in THE JOURNAL OF PHYSICAL CHEMISTRY A · MAY 2007

Impact Factor: 2.69 · DOI: 10.1021/jp067587+ · Source: PubMed

CITATIONS

14

READS

24

2 AUTHORS:



Robert L. Waterland

Dupont

32 PUBLICATIONS 638 CITATIONS

SEE PROFILE



Kerwin D. Dobbs

Dupont

47 PUBLICATIONS 2,304 CITATIONS

SEE PROFILE

Atmospheric Chemistry of Linear Perfluorinated Aldehydes: Dissociation Kinetics of $C_nF_{2n+1}CO$ Radicals

Robert L. Waterland* and Kerwin D. Dobbs

DuPont Central Research & Development, Experimental Station, P. O. Box 80320,
Wilmington, Delaware 19880-0320

Received: November 15, 2006; In Final Form: January 22, 2007

Linear perfluorinated aldehydes (PFALs, $C_nF_{2n+1}CHO$) are important intermediate species in the atmospheric oxidation pathway of many polyfluorinated compounds. PFALs can be further oxidized in the gas phase to give perfluorinated carboxylic acids (PFCAs, $C_nF_{2n+1}C(O)OH$, $n = 6, 12$) which have been detected in animal tissues and at low parts per billion levels in human blood sera. In this paper, we report ab initio quantum chemistry calculations of the decarbonylation kinetics of $C_nF_{2n+1}CO$ radicals. Our results show that $C_nF_{2n+1}CO$ radicals have a strong tendency to decompose to give C_nF_{2n+1} and CO under atmospheric conditions: the Arrhenius activation energies for decarbonylation of CF_3CO , C_2F_5CO , and C_3F_7CO obtained using PMP4/6-311++G(2d,p) are 8.8, 6.6, and 5.8 kcal/mol, respectively, each of which is about 5 kcal/mol lower than the barrier for the corresponding nonfluorinated radicals. The lowering of the barrier for decarbonylation of $C_nF_{2n+1}CO$ relative to that of $C_nH_{2n+1}CO$ is well explained by electron withdrawal by F atoms that serve to weaken the critical C–CO bond. These results have important implications for the atmospheric fate of PFALs and the atmospheric pathways to PFCAs. The main effect of decarbonylation of $C_nF_{2n+1}CO$ is to decrease the molar yield of $C_nF_{2n+1}C(O)OH$; if 100% of the $C_nF_{2n+1}CO$ decompose, the yield of $C_nF_{2n+1}C(O)OH$ must be zero. There is considerable scope for additional experimental and theoretical studies.

1. Introduction

In the past decade, a variety of highly persistent polyfluorinated anionic species have been detected in humans and animals^{1–14} in both urban and remote locations. In almost all of these studies, perfluorooctanesulfonate (PFOS, $C_8F_{17}SO_3^-$) was the most abundant anion found, but related species such as perfluorooctanoate (PFO, $C_7F_{15}COO^-$), perfluorononanoate (PFN, $C_8F_{17}COO^-$), and perfluorohexanesulfonate ($C_6F_{13}SO_3^-$) and neutral species such as perfluorooctane sulfonamide ($C_8F_{17}SO_3NH_2$) were also detected.

The observation of long-chain perfluoroalkyl anions in Arctic biota far from industrial sources and large population centers puzzled early investigators:^{15,16} these species were manufactured and used primarily in temperate zones and must have been transported to the Arctic. Such transport was said to be unlikely given the high aqueous solubility of anions and the low volatility of the corresponding salts. Hence, it was hypothesized that one or more volatile fluorinated precursor molecules were responsible for the perfluoroalkyl anions observed in Arctic biota.^{17,18} These precursors were presumed to be slowly oxidized by atmospheric radical species to give fluorinated acids which would be deposited in the Arctic by precipitation.

Fluorotelomer alcohols (FTOHs, $C_nF_{2n+1}CH_2CH_2OH$) were the first molecular class to be proposed as precursors for perfluorinated carboxylic acids (PFCAs, $C_nF_{2n+1}C(O)OH$), and FTOHs were subsequently detected in low concentration in the northern hemispheric troposphere.^{19,20} In addition, laboratory photoreactor studies identified a plausible pathway from FTOHs to the corresponding PFCAs, although the atmospheric yield of such acids is a focus of ongoing study.^{18,21} Later studies

identified other potential acid precursors including fluorotelomer olefins²² (FTOs, $C_nF_{2n+1}CH=CH_2$) and *N*-alkyl perfluoroalkyl-sulfonamidoethanols (PFSEs, $C_nF_{2n+1}SO_2N(CH_3)CH_2CH_2OH$).²³ Interestingly, photoreactor studies²³ have indicated that PFSEs may contribute to the observed environmental burden of both perfluoroalkyl sulfonates and carboxylate compounds.

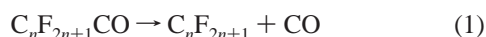
Considerable uncertainty surrounds the atmospheric precursor hypothesis. First, the physicochemical properties and partitioning behavior of some of the proposed precursors and many of their degradation products are often poorly determined.^{24–28} Second, the interpretation of photoreactor studies in the larger atmospheric context is a nontrivial task. Use of global and regional scale three-dimensional tropospheric fate models is extremely useful in this regard, but to date these have only been applied to FTOH chemistry.^{29,30} Finally, the initial view that long-chain perfluoroalkyl anions are static in the environment is flawed: ocean transport has been shown to be important for persistent organic pollutants with low Henry's law constants. For example, the Henry's law constant at 25 °C for the β -isomer of hexachlorocyclohexane (β -HCH) is almost 8 times lower than that of the α -isomer.³¹ Accordingly, β -HCH is more efficiently scavenged by precipitation, is enriched in seawater relative to α -HCH, and is preferentially deposited closer to its source regions in Asia.³² Ocean currents then transport β -HCH north into the Bering Sea via the Bering Strait. PFO and other perfluorocarboxylate anions are highly water soluble and have no appreciable vapor pressure, so their Henry's law constants are substantially lower than that of β -HCH. Thus, it is likely that oceanic transport of primary acid emissions plays a significant role in transport of long-chain perfluorocarboxylates to the Arctic.

Nevertheless, the atmospheric oxidation of precursors clearly accounts for some fraction of the observed burden of PFCAs

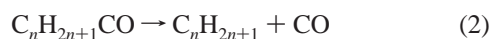
* Corresponding author. E-mail: Robert.L.Waterland@usa.dupont.com.

in remote regions. As established by experimental studies, the estimated atmospheric lifetimes of FTOHs (12–20 days),^{17,33} FTOs (8 days),^{22,34} and a major degradation product of PFSEs (20–50 days)²³ permit their transport to remote regions. Of particular interest to the present study, FTOHs and FTOs produce linear perfluorinated aldehydes (PFALs, $C_nF_{2n+1}CHO$) as primary oxidation products in photoreactor experiments.^{34,35} PFALs, which are important intermediate species in the atmospheric oxidation pathway of many polyfluorinated compounds, are stable species with estimated atmospheric lifetimes of about 20 days.^{36,37} PFALs are the critical link to perfluorinated acids in the oxidation mechanisms proposed by Ellis et al.¹⁸ for FTOHs and by Wallington³⁸ for FTOs. Thus, the physical and chemical properties of PFALs clearly control the yield of PFCAs produced from precursors. To date, the few experimental and theoretical studies of the chemical properties of PFALs which do exist are sometimes contradictory.^{36,39} This paper is the first in a series which will examine important aspects of the atmospheric fate of PFALs using ab initio quantum chemistry methods.

1.1. Computational Models. We have examined the high-pressure limit gas-phase decarbonylation of a homologous series of perfluoroacyl radicals via reaction 1



and the corresponding reaction for nonfluorinated species:



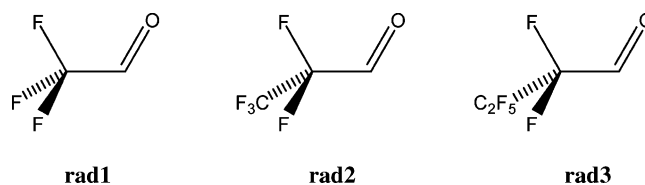
These reactions compete with the combination reaction with molecular oxygen to form perfluoroacyl peroxy and acyl peroxy radicals via reactions 3 and 4:



Solignac et al.⁴⁰ recently measured a CO yield of $61 \pm 2\%$ in the Cl atom initiated oxidation of C_3F_7CHO at 298 K and 1000 mbar pressure of air. Since C_3F_7CO is the only primary product of the reaction of C_3F_7CHO with Cl, the decarbonylation of C_3F_7CO radicals in air via reaction 1 must compete very effectively with addition of molecular oxygen via reaction 3. Very recently, Hurley et al.⁴¹ have reported that 2%, 52%, 81%, and 89% of $C_nF_{2n+1}CO$ radicals decompose to C_nF_{2n+1} radicals and CO for $n = 1, 2, 3$, and 4, respectively. These results are in sharp contrast to the available experimental data for linear $C_nH_{2n+1}CO$ radicals which nearly exclusively add O_2 via reaction 4 rather than decompose via reaction 2.⁴² In the oxidation mechanisms proposed to date, reactions 1 and 3 are the beginning of pathways that lead, in part, to perfluorinated acids, and the competition between these reactions can significantly influence PFCA yields. Examining the properties of perfluoroacyl radicals and their better studied nonfluorinated radical analogues with ab initio methods provides insight into the source of the differences observed in their chemical fate.

2. Methodology

The ab initio calculations were performed using the Gaussian 03 suite of programs⁴³ and the GaussView program.⁴⁴ We considered reaction 1 for the three smallest perfluoroacyl radicals CF_3CO , C_2F_5CO , and C_3F_7CO shown here as **rad1**, **rad2**, and **rad3**.



In addition, we examined the analogous reactions for non-fluorinated species. Ground state geometries of these radicals, the corresponding products of reactions 1 and 2, and all transition states were obtained using second-order Møller–Plesset perturbation theory^{45,46} (MP2) in conjunction with the 6-31G(d) basis set.⁴⁷ Throughout this work, we used the frozen-core approximation in all post-SCF electron correlation methods. Stationary points on the potential surface were characterized as minima or transition states by determination of harmonic vibrational frequencies using analytic second derivatives at the same level of theory. All transition states were characterized by a single imaginary frequency. The zero-point energy and thermodynamic functions were determined using the calculated frequencies scaled by 0.9434,⁴⁸ and all normal modes were treated as vibrations. We have shown **rad2** and **rad3** in their energetically preferred C_1 conformations where the $C=O$ bond eclipses a $C-F$ bond rather than a $C-C$ bond. In **rad1** the $C=O$ bond also eclipses a $C-F$ bond and the radical has C_s symmetry. The transition states show this same pattern: $[C_2F_5\cdots CO]^\ddagger$ and $[C_3F_7\cdots CO]^\ddagger$ have C_1 symmetry, $[CF_3\cdots CO]^\ddagger$ has C_s symmetry, and in all cases the $C=O$ bond eclipses a $C-F$ bond. The corresponding nonfluorinated radicals are all of C_s symmetry with the $C=O$ bond eclipsing a $C-C$ bond.

There are no experimental geometries for the perfluorinated radicals studied in this work, but previous work on closed-shell fluorinated species show that polarization functions on heavy atom centers are essential⁴⁹ while the addition of diffuse functions has little effect on the accuracy of computed geometries.⁵⁰ The level of theory we have employed has been shown to give accurate structures for closed-shell fluorinated systems.⁵¹

Single-point energy calculations were performed on the MP2 optimized geometries using fourth-order Møller–Plesset perturbation theory with single, double, triple, and quadruple substitutions (MP4SDTQ).⁵² We estimated the effect of diffuse functions on reaction barriers and thermodynamics by using the 6-311G(2d) and 6-311+G(2d) basis sets for fluorinated species and the 6-311G(2d,p) and 6-311++G(2d,p) basis sets for nonfluorinated species.⁵³ For open-shell species, we performed unrestricted calculations and also examined the effects of spin projection on estimated barriers.

3. Results and Discussion

3.1. Geometries and Harmonic Vibrational Frequencies. Computed UMP2/6-31G(d) structures of the $C_nF_{2n+1}CO$ radicals and the corresponding transition states are provided as Supporting Information. The most important structural parameters, the $C=O$ and the $C-CO$ bond lengths in the radicals and the transition states, are summarized in Table 1.

The $C=O$ bond lengths of the radicals and the transition states are independent of the length of the perfluoroalkyl chain. The $C-CO$ bond in the radicals lengthens slightly as the number of CF_2 units increase. There is a more marked decrease in the $C-CO$ bond length for the transition states. These changes are indicative of a weakening of the $C-CO$ bond as the perfluoroalkyl chain lengthens. There is a corresponding modest increase in the magnitude of the imaginary frequency of the breaking $C-C$ bond. The transition state $[CF_3\cdots CO]^\ddagger$ for decarbonylation

TABLE 1: UMP2/6-31G(d) Bond Lengths (Å) for $C_nF_{2n+1}CO$ Radicals and Transition States

	C=O		C–CO	
	radical	TS	radical	TS
CF ₃ CO (rad1)	1.186	1.161	1.552	2.071
C ₂ F ₅ CO (rad2)	1.187	1.161	1.555	2.054
C ₃ F ₇ CO (rad3)	1.187	1.161	1.559	2.053

of **rad1** has an unscaled imaginary frequency of 448.6i cm⁻¹, while the transition states for **rad2** and **rad3** decarbonylation have unscaled imaginary frequencies of 463.0i and 462.1i cm⁻¹, respectively.

There are no experimental geometries or frequencies to which we can compare our results, but there are several previous theoretical studies for **rad1** and [CF₃...CO][‡]. Francisco and Abersold⁵⁴ computed the geometry of **rad1** using UMP2/6-31G(d) and UMP2/6-311G(d). Their UMP2/6-31G(d) geometry agrees with the values in Table 1 to within 0.002 Å. With UMP2/6-311G(d), the C=O bond length is 1.176 Å and the C–CO bond length is 1.556 Å; these bond lengths are, respectively, 0.01 Å shorter and 0.004 Å longer than our results. Francisco⁵⁵ computed the geometry of [CF₃...CO][‡] using UMP2/6-31G(d) and also reported unscaled harmonic frequencies of [CF₃...CO][‡] at the UHF/6-31G(d) level of theory. The UMP2/6-31G(d) geometry agrees with Table 1 to within 0.002 Å, and the transition state harmonic frequency is 500i cm⁻¹. Maricq et al.⁵⁶ computed the harmonic frequencies of [CF₃...CO][‡] using UMP2/6-31G(d) and obtained a transition state harmonic frequency of 446i cm⁻¹, which is indistinguishable from our value. Méreau et al.⁶⁴ calculated geometries for **rad1** and [CF₃...CO][‡] using MP2(full)/6-31G(d), and their C=O and C–CO bond lengths agree with ours to within 0.002 Å, showing that the frozen-core approximation we have used produces no significant change in the computed geometries. Viskolcz and Bérces⁵⁷ also report an MP2(full)/6-31G(d) geometry for **rad1** which agrees with that from Méreau et al. to within 0.001 Å. The tiny differences in the reported MP2/6-31G(d) geometries are probably due to slightly varying convergence criteria for the optimizations and the effects of frozen-core approximations.

3.2. Energetics and Kinetics. The computed activation energies (ΔE^\ddagger) and energies of reaction (ΔE_r) for reaction 1 for the cases $n = 1, 2, 3$ are given in Table 2. The individual energies of the reactants, transition states, and products are provided as Supporting Information.

ΔE^\ddagger for decarbonylation of **rad1** ranges from a maximum of 15.3 kcal/mol for UMP2/6-31G(d)//UMP2/6-31G(d) to a minimum of 9.8 kcal/mol for PMP4/6-311G(2d)//UMP2/6-31G(d). As one would expect, changing from a double- ζ (PMP2/6-31G(d)) to a triple- ζ basis (PMP2/6-311G(2d)) reduces the activation energy, in this case from 13.2 kcal/mol to 11.5 kcal/mol. Interestingly, the addition of diffuse functions to the basis has almost no effect on the computed activation energy. Spin contamination is apparent for the open-shell species in the decarbonylation of **rad1**. For example, the UMP2/6-31G(d) wave functions of **rad1**, CF₃, and [CF₃...CO][‡] have S^2 expectation values of 0.771, 0.754, and 0.812, respectively.

The activation energy for decarbonylation of larger perfluoroacyl radicals is smaller than that for **rad1**. Our best estimates are based on PMP4/6-311+G(2d). At this level of theory, the decarbonylation activation energies for **rad1**, **rad2**, and **rad3** are 10.1, 7.9, and 7.1 kcal/mol, respectively. If we focus on the breaking C–C bond, the largest change in chemical environment occurs in going from CF₃CO to C₂F₅CO. Further lengthening of the perfluorinated tail might be expected to have

a limited effect. Correspondingly, the change in the activation energy is larger in going from CF₃CO to C₂F₅CO than from C₂F₅CO to C₃F₇CO, and in each case the effect reduces the barrier for decarbonylation. Francisco⁵⁵ reported ΔE^\ddagger for decarbonylation of **rad1** as 13.5 kcal/mol using PMP2(full)/6-31G(d), which is very close to our PMP2(fc)/6-31G(d) value of 13.2 kcal/mol. There are no published ΔE^\ddagger values for decarbonylation of larger perfluoroacyl radicals. Significant spin contamination is observed for some of the open-shell species in reaction 1. In particular, the transition state wave functions have up to 9% spin contamination before annihilation of unwanted spin states. This level of spin contamination can lead to substantial errors in energetics,⁵⁸ so it is essential to adopt spin-projection methods. For all the species we studied, spin projection is very effective in eliminating the higher spin components; i.e., the expectation value of S^2 is very close to 3/4 after the spin-projection procedure.

The results we obtained for the decarbonylation of acyl radicals (reaction 2) are given in Table 3. The activation energies for reaction 2 at the PMP4/6-311++G(2d,p)//UMP2/6-31G(d) level of theory for CH₃CO, C₂H₅CO, and C₃H₇CO are 15.7, 14.1, and 14.5 kcal/mol, respectively. Each is 5–7 kcal/mol higher than that for the corresponding perfluoroacyl radical reaction, indicating that $C_nF_{2n+1}CO$ radicals decarbonylate much more readily than the corresponding $C_nH_{2n+1}CO$ radicals.

Adding thermal and zero-point energy corrections does not change this picture. Activation energies E_a for reactions 1 and 2 at temperature T were calculated from $E_a = \Delta H^\ddagger(T) + RT$, where the enthalpy of activation, $\Delta H^\ddagger(T)$, included the zero-point-energy level and thermal corrections at temperature T . The Arrhenius activation energies E_a at 298.15 K obtained using PMP4/6-311++G(2d,p)//UMP2/6-31G(d) are given in Table 4. $E_a(298.15\text{ K})$ and ΔE^\ddagger show the same trends: $E_a(298.15\text{ K})$ is lower for the longer perfluoroacyl and acyl radicals. $E_a(298.15\text{ K})$ for **rad2** is 2.1 kcal/mol lower than that of **rad1**, and the barrier is further slightly reduced for **rad3**. The computed barrier for **rad3** is quite modest (5.8 kcal/mol). $E_a(298.15\text{ K})$ for decarbonylation of C₂H₅CO is likewise 2.0 kcal/mol lower than that of CH₃CO but is slightly higher for C₃H₇CO. Again, the major change in Arrhenius activation energies occurs in going from the smallest homologues (**rad1** and CH₃CO) to the next larger homologues (**rad2** and C₂H₅CO).

Our results indicate that longer perfluoroacyl and acyl radicals have an increased propensity to decarbonylate. This effect has been seen experimentally for CH₃CO and C₂H₅CO. Our results should be compared to experimental Arrhenius activation energies obtained by extrapolation to the high-pressure limit. The extrapolated experimental $E_a(298.15\text{ K})$ for CH₃CO⁵⁹ is 2.8 kcal/mol higher than that of C₂H₅CO,⁶⁰ which agrees quite well with our difference of 2.0 kcal/mol. However, our absolute $E_a(298.15\text{ K})$ values obtained with PMP4/6-311+G(2d)//UMP2/6-31G(d) are substantially lower than those obtained by extrapolating the experimental results to the high-pressure limit. It is unclear why our computed results are lower than the extrapolated $E_a(298.15\text{ K})$ obtained in some experimental studies, but as noted by Watkins and Thompson⁶⁰ and Tomas et al.,⁶¹ the experiments generally involve complex free-radical systems with many competing reactions and, since most of the data are obtained far from the high-pressure limit, the extrapolation to infinite pressure is somewhat uncertain. We also note that O'Neal and Benson⁶² gave an extrapolated experimental $E_a(298.15\text{ K})$ for CH₃CO decarbonylation of 15.0 kcal/mol and Barnes et al.⁶³ reported the barrier for CF₃CO decarbonylation

TABLE 2: Computed Activation Energies (ΔE^\ddagger) and Reaction Energies (ΔE_r) in kcal/mol for $C_nF_{2n+1}CO \rightarrow C_nF_{2n+1} + CO$ for $n = 1-3$

	$CF_3CO \rightarrow CF_3 + CO$		$C_2F_5CO \rightarrow C_2F_5 + CO$		$C_3F_7CO \rightarrow C_3F_7 + CO$	
	ΔE^\ddagger^a	ΔE_r^a	ΔE^\ddagger^a	ΔE_r^a	ΔE^\ddagger^a	ΔE_r^a
UMP2/6-31G(d)	15.3	7.0	13.3	5.8	12.7	5.3
PMP2/6-31G(d)	13.2	8.3	11.2	7.0	10.5	6.4
PMP2/6-311G(2d)	11.5	6.8	9.7	5.8	8.8	5.0
PMP2/6-311+G(2d)	11.8	7.4	9.8	5.9	8.9	5.1
UMP4/6-311G(2d)	11.4	4.3	9.5	3.2	8.6	2.5
UMP4/6-311+G(2d)	11.6	4.9	9.5	3.3	8.7	2.6
PMP4/6-311G(2d)	9.8	5.1	7.8	3.8	7.0	3.1
PMP4/6-311+G(2d)	10.1	5.8	7.9	4.0	7.1	3.3

^a ΔE^\ddagger is the electronic energy difference between $[C_nF_{2n+1}\cdots CO]^\ddagger$ and $C_nF_{2n+1}CO$ excluding zero-point energy differences or thermal effects. ΔE_r is the electronic energy difference between $C_nF_{2n+1} + CO$ and $C_nF_{2n+1}CO$ and also excludes zero-point energy differences or thermal effects.

TABLE 3: Computed Activation Energies (ΔE^\ddagger) and Reaction Energies (ΔE_r) in kcal/mol for $C_nH_{2n+1}CO \rightarrow C_nH_{2n+1} + CO$ for $n = 1-3$

	$CH_3CO \rightarrow CH_3 + CO$		$C_2H_5CO \rightarrow C_2H_5 + CO$		$C_3H_7CO \rightarrow C_3H_7 + CO$	
	ΔE^\ddagger^a	ΔE_r^a	ΔE^\ddagger^a	ΔE_r^a	ΔE^\ddagger^a	ΔE_r^a
UMP2/6-31G(d,p)	21.3	12.8	19.9	12.8	20.1	13.5
PMP2/6-31G(d,p)	18.8	13.0	17.4	12.8	17.7	13.6
PMP2/6-311G(2d,p)	17.2	11.7	15.8	11.7	16.3	12.5
PMP2/6-311++G(2d,p)	18.2	12.7	16.6	12.5	17.0	13.3
UMP4/6-311G(2d,p)	16.6	8.8	15.1	8.7	15.5	9.4
UMP4/6-311++G(2d,p)	17.6	9.9	15.9	9.5	16.3	10.2
PMP4/6-311G(2d,p)	14.7	8.9	13.3	8.7	13.7	9.4
PMP4/6-311++G(2d,p)	15.7	10.0	14.1	9.6	14.5	10.3

^a ΔE^\ddagger is the electronic energy difference between $[C_nH_{2n+1}\cdots CO]^\ddagger$ and $C_nH_{2n+1}CO$ excluding zero-point energy differences or thermal effects. ΔE_r is the electronic energy difference between $C_nH_{2n+1} + CO$ and $C_nH_{2n+1}CO$ and also excludes zero-point energy differences or thermal effects.

TABLE 4: Computed Activation Energies in kcal/mol at 298.15 K Obtained Using PMP4/6-311++G(2d,p) on UMP2/6-31G(d) Geometries and $E_a(T) = \Delta H^\ddagger(T) + RT$

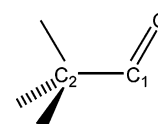
	$E_a(298.15\text{ K})$
$CF_3CO \rightarrow CF_3 + CO$	8.7
$C_2F_5CO \rightarrow C_2F_5 + CO$	6.6
$C_3F_7CO \rightarrow C_3F_7 + CO$	5.8
$CH_3CO \rightarrow CH_3 + CO$	13.7
$C_2H_5CO \rightarrow C_2H_5 + CO$	11.7
$C_3H_7CO \rightarrow C_3H_7 + CO$	12.2

of 9.8 ± 2.4 kcal/mol, which are quite close to our calculated values of 13.7 and 8.7 kcal/mol, respectively.

There is a disparity between our results and the barriers obtained by Méreau et al.⁶⁴ using the G2(MP2) method. Méreau et al.⁶⁴ reported $E_a(298.15\text{ K})$ for decarbonylation of the acetyl radical as 17.3 kcal/mol, which agrees extraordinarily well with the extrapolated $E_a(298.15\text{ K})$ value of 17.2 kcal/mol obtained by Watkins and Word.⁵⁹ Since our value of 13.7 kcal/mol is 3.6 kcal/mol lower than that of Méreau et al.,⁶⁴ we first repeated their calculations and confirmed their results and also performed additional calculations for decarbonylation of CH_3CO with two other correlated methods, namely QCISD(T)/6-311G(d)//UMP2/6-31G(d) and CCSD(T)/6-311++G(2d,p)//UMP2/6-31G(d). The $E_a(298.15\text{ K})$ values obtained were 14.3 kcal/mol (QCISD(T)/6-311G(d)) and 14.7 kcal/mol (CCSD(T)/6-311++G(2d,p)), which are significantly closer to our PMP4/6-311++G(2d,p)//UMP2/6-31G(d) than to those of Méreau et al.⁶⁴ The remaining difference between our results and those obtained using QCISD(T) and CCSD(T) are probably due to spin contamination. $E_a(298.15\text{ K})$ was 15.5 kcal/mol using UMP4/6-311++G(2d,p)//UMP2/6-31G(d) (no spin projection), which agrees well with the CCSD(T)/6-311++G(2d,p)//UMP2/6-31G(d) value of 14.7 kcal/mol. Spin projection is not available in the G2(MP2), QCISD(T), and CCSD(T) methods, so we believe the results reported in Table 4 are the best computational barriers obtained to date.

Turning now to the relative barriers for $C_nF_{2n+1}CO$ and $C_nH_{2n+1}CO$ radicals, we see that $E_a(298.15\text{ K})$ is at least 5 kcal/mol lower for the perfluoroacyl radicals. If we ignore the generally modest differences in the frequency factor, reducing $E_a(298.15\text{ K})$ by 5 kcal/mol will increase the Arrhenius rate constant by a factor of about 5000. Our results are entirely consistent with the large CO yields measured by Solignac et al.⁴⁰ and Hurley et al.⁴¹ for the Cl atom initiated oxidation of $C_nF_{2n+1}CHO$.

What is the physical origin of the lowering of the barrier of $C_nF_{2n+1}CO$ relative to $C_nH_{2n+1}CO$? As is often the case in quantum chemistry, cause and effect are difficult to deconvolve, but an important clue is that the C–CO bond in $C_nF_{2n+1}CO$ radicals is about 0.04 Å longer than the corresponding bond in $C_nH_{2n+1}CO$ radicals. A further clue comes from Mulliken⁶⁵ and NBO⁶⁶ population analysis of the UMP2/6-31G(d,p) wave functions for the radicals. The Mulliken and NBO population analyses give entirely consistent results, and for completeness, we have provided the NBO results as Table S7 in the Supporting Information. Previous work has shown that useful insight can be obtained by calculating changes in Mulliken partial charges after atomic substitution.⁶⁷ The C–CO bond lengths and the results of the Mulliken population analysis for the critical C_1 , C_2 , and O atoms (see figure below) of $C_nF_{2n+1}CO$ and $C_nH_{2n+1}CO$ radicals are given in Table 5.



Inspecting Table 5, we see that fluorination and increasing molecular size have a quite modest effect on the partial electronic charges on the C_1 and O atoms. In contrast, the highly electronegative F atoms in $C_nF_{2n+1}CO$ withdraw substantial electronic charge from the C_2 atom. The inductive effect is

TABLE 5: C–CO Bond Lengths (Å), Partial Charges^a $q(C_1)$, $q(C_2)$, and $q(O)$ on Critical Carbon and Oxygen Atoms, Total Overlap Populations $p(C_1, C_2)$ between C_1 and C_2 Atoms, and Charge Products $q(C_1) q(C_2)$ of $C_nX_{2n+1}CO$ Radicals for $X = H$, F and $n = 1–3$ Obtained by Mulliken Population Analysis of the UMP2/6-31G(d,p) Wave Functions

	C–CO	$q(C_1)$	$q(C_2)$	$q(O)$	$p(C_1, C_2)$	$q(C_1) q(C_2)$
CF ₃ CO (rad1)	1.552	0.188	0.844	−0.225	0.479	0.159
CH ₃ CO	1.514	0.249	−0.422	−0.283	0.403	−0.105
C ₂ F ₅ CO (rad2)	1.555	0.219	0.517	−0.217	0.284	0.113
C ₂ H ₅ CO	1.519	0.250	−0.310	−0.286	0.383	−0.078
C ₃ F ₇ CO (rad3)	1.559	0.231	0.555	−0.216	0.327	0.128
C ₃ H ₇ CO	1.519	1.251	−0.311	−0.285	0.387	−0.078

^a In atomic units (charge on a free electron is −1.00).

strongest for CF₃CO, where three F atoms are bonded to C₂ and together withdraw about 1.3 electrons relative to CH₃CO. In C₂F₅CO and C₃F₇CO, only two F atoms are bonded to the C₂ atom and together they withdraw about 0.8 electron relative to C₂H₅CO and C₃F₇CO. In Table 5 we have separated the net charge contributions to the C–CO bond into covalent (overlap population, $p(C_1, C_2)$) and electrostatic contributions ($q(C_1) q(C_2)$). There are no obvious trends in $p(C_1, C_2)$ but we see that the electrostatic charge product $q(C_1) q(C_2)$ is negative (attractive) for $C_nH_{2n+1}CO$ radicals and positive (repulsive) for $C_nF_{2n+1}CO$ radicals. We conclude that the main effect of electron withdrawal in $C_nF_{2n+1}CO$ is to increase the electrostatic repulsion between C₁ and C₂ and to weaken the critical C–CO bond.

3.3. Atmospheric Consequences. The chamber experiment of Ellis et al.¹⁸ produced a homologous series of PFCAs that were formed in small yields during the simulated atmospheric oxidation of 8:2 fluorotelomer alcohol (8:2 FTOH, C₈F₁₇CH₂CH₂OH). Chemical degradation of 8:2 FTOH in the chamber was initiated by Cl atoms rather than OH radicals, and the Ellis et al.¹⁸ experiment was performed without NO to emphasize the role of peroxy radical reactions that are believed responsible for PFCA production. The initial steps in the FTOH reaction mechanism are well established,³³ and they lead in turn to the 8:2 telomer aldehyde (C₈F₁₇CH₂CHO) and the 8:2 perfluorinated aldehyde (C₈F₁₇CHO). After 94% conversion of 8:2 FTOH, Ellis et al.¹⁸ measured a yield of C₈F₁₇C(O)OH (PFNA) of 1.6%. A homologous series of shorter PFCAs were also identified with diminishing yields of 1.5% (C₇F₁₅C(O)OH, PFOA), 0.32% (C₆F₁₃C(O)OH, PFHpA), 0.24% (C₅F₁₁C(O)OH, PFHxA), and 0.1% (C₄F₉C(O)OH, PFPA).

To explain these findings, Ellis et al.¹⁸ and Andersen et al.⁶⁸ proposed a chemical mechanism which begins with the formation of a perfluoroacyl radical, C₈F₁₇CO. For PFNA production, they adapted a well-known mechanism from the hydrocarbon chemistry literature.⁶⁹ This scheme has the following steps:



In reaction 6, M represents a nitrogen or oxygen molecule; reaction 3 is the infinite-pressure limit form of reaction 6. The C₈F₁₇C(O)O₂ radicals produced by reaction 6 react with HO₂ radicals to produce PFNA (reaction 7a), the corresponding peracid (reaction 7b), and C₈F₁₇C(O)O radicals (reaction 7c). Note that this scheme incorporates the addition of molecular oxygen to C₈F₁₇CO but neglects the competing decarbonylation

reaction of C₈F₁₇CO. This is an important omission since decarbonylation of C₈F₁₇CO to give C₈F₁₇ radicals and CO disrupts this scheme: there is no pathway to the nine-carbon species PFNA from the eight-carbon C₈F₁₇ radical.

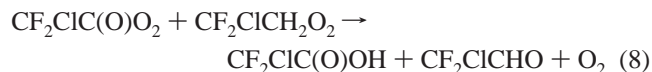
Support for the Ellis et al.¹⁸ pathway to PFNA (reactions 5–7) comes primarily from a series of experiments in which shorter chain perfluorinated aldehydes were reacted with Cl atoms in 700 Torr of air at 298 K. For the reaction of C₂F₅CHO with Cl in the absence of NO, Andersen et al.⁷⁰ found a molar yield of 24% for C₂F₅C(O)OH, inferred a branching ratio of 76% for C₂F₅C(O)O, and found no evidence of C₂F₅C(O)OOH production. With NO present, C₂F₅C(O)OH was not evident in the product spectra.⁷¹ Subsequent experiments⁶⁸ in the same chamber found progressively smaller molar PFCA yields of 38%, 10%, and 8% for reaction of Cl atoms with CF₃CHO, C₃F₇CHO, and C₄F₉CHO, respectively. As noted by the authors, the 14% yield difference of C₂F₅C(O)OH and C₃F₇C(O)OH is difficult to explain.

In each of these papers, it was assumed that reaction with O₂ was the sole fate of $C_nF_{2n+1}CO$ radicals. Our calculations and the experiments of Solignac et al.⁴⁰ and Hurley et al.⁴¹ show that this assumption was incorrect. The authors of Ellis et al.¹⁸ and Andersen et al.⁶⁸ have subsequently recognized their error, and in their most recent paper⁴¹ they reported the CO yields during the Cl atom initiated oxidation of $C_nF_{2n+1}CHO$ in the presence of NO and varying partial pressures of O₂. As noted above, 2%, 52%, 81%, and 89% of $C_nF_{2n+1}CO$ radicals decompose to C_nF_{2n+1} radicals and CO for $n = 1, 2, 3$, and 4, respectively. To retain the reaction scheme (reactions 5–7) they had previously proposed, Hurley et al.⁴¹ increased the PFCA yields found in their earlier work to account for the fraction of $C_nF_{2n+1}CO$ that decompose. For example, the yield of C₄F₉C(O)OH from the reaction of C₄F₉CHO with Cl atoms in the presence of HO₂ was previously reported⁶⁸ as $8 \pm 2\%$. Since the yield of C₄F₉C(O)O₂ radicals is 11%, the adjusted yield of C₄F₉C(O)OH is $0.08/0.11 = 73\%$. Thus, incorporating perfluoroacyl radical decomposition increases the branching ratio of reaction 7a by an order of magnitude. In addition, the adjusted yields of $C_nF_{2n+1}C(O)OH$ from the reaction of $C_nF_{2n+1}CHO$ with Cl atoms show a strongly increasing trend: the yields are $39 \pm 4\%$, $50 \pm 8\%$, $53 \pm 11\%$, and $73 \pm 18\%$ for $n = 1, 2, 3$, and 4, respectively.

The existing literature on reactions of R_FC(O)O₂ and R_HC(O)O₂ radicals with HO₂ is meager. The 2006 IUPAC compilation⁷² (available online at <http://www.iupac-kinetic.ch.cam.ac.uk/>) contains only one such reaction, that of CH₃C(O)OO with HO₂. In this case, the yield of CH₃C(O)OH is $\leq 20\%$, which is not unreasonably different from the adjusted yield of $39 \pm 4\%$ for CF₃C(O)OO with HO₂ reported by Hurley et al.⁴¹ However, there is no support in the literature for yields in excess of 70% in the reactions of acyl or fluoroacyl peroxy radicals with HO₂. In addition, the available literature indicates that the corresponding reaction of R_FO₂ radicals with HO₂ to give R_FOH does

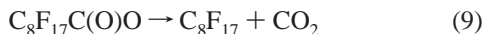
not occur. For example, CF_3CHFO_2 reacts with HO_2 to give the peroxide CF_3CHFOOH and O_2 in unit yield.⁷²

We have seen that incorporating radical decomposition directly into the Ellis et al.¹⁸ pathway to PFNA leads to yields that are hard to reconcile with the literature. This suggests that one or more additional pathways to PFNA are missing from the Ellis et al.¹⁸ scheme. An example of such a pathway can be found in the work of Tuazon and Atkinson,⁷³ which showed the oxidation of CF_2ClCH_3 with Cl atoms in the presence of air produced an aldehyde which is very similar to the ones we have been studying. Subsequent oxidation of this aldehyde produced a perhalogenated acid ($\text{CF}_2\text{ClC}(\text{O})\text{OH}$) in sizable yield and, most significantly, a fraction of the acid production results from the radical–radical reaction



Note that this reaction also regenerates the aldehyde which further complicates the analysis. Radicals of these types were present in the Ellis et al.¹⁸ experiment, and there seems, in retrospect, little reason to exclude this mechanism. In the atmosphere the important peroxy radical would be CH_3O_2 .

As we noted above, the Ellis et al.¹⁸ chamber experiment produced a homologous series of lower PFCAs (PFOA, PFHpA, PFHx, and PFPA) in small yields. These lower acids, which must be produced by a different mechanism from PFNA, are nevertheless also strongly influenced by decomposition of perfluoroacyl radicals. The $\text{C}_8\text{F}_{17}\text{C}(\text{O})\text{O}$ radicals produced by reaction 7c would be expected to decarboxylate promptly⁵⁵ and add molecular oxygen to give perfluoroperoxy radicals $\text{C}_8\text{F}_{17}\text{O}_2$:



In the chamber, the dominant fate of $\text{C}_8\text{F}_{17}\text{O}_2$ is reaction with HO_2 and other RO_2 radicals to produce a so-called “unzipping” cascade that produces eight CF_2O molecules from each $\text{C}_8\text{F}_{17}\text{O}_2$ radical. $\text{C}_8\text{F}_{17}\text{O}_2$ radicals can also be produced by direct photodissociation of $\text{C}_8\text{F}_{17}\text{CHO}$ or by the addition of O_2 to the C_8F_{17} radicals produced from reaction 6. These steps are well supported in the hydrocarbon and hydrofluorocarbon literature, but as we have seen, the branching ratio for reaction 7c is dependent on the degree to which $\text{C}_8\text{F}_{17}\text{CO}$ decomposes.

From this point, Ellis et al.¹⁸ proposed a novel competing pathway to the lower PFCAs that begins with the reaction of $\text{C}_8\text{F}_{17}\text{O}_2$ and an α -dihydrogenated peroxy radical RH_2O_2 to give an unstable α -fluoro alcohol. This pathway contains the following steps:



Reaction 12 occurs rapidly on any surface, and the $\text{C}_7\text{F}_{15}\text{CFO}$ product will hydrolyze to give $\text{C}_7\text{F}_{15}\text{C}(\text{O})\text{OH}$ (PFOA). This ingenious mechanism is essentially unsupported in the literature. To the best of our knowledge, there have been no experiments in which a fluorinated peroxy radical reacts with an α -dihydrogenated peroxy radical, but similar experiments that examine the self-reaction of α -hydrogenated fluoroperoxy radicals indicate that reaction 11 has, at best, a very small yield. The self-reaction of CHF_2O_2 produces no CHF_2OH ,⁷⁴ and the preferred value of the CH_2FOH yield in the self-reaction of

CH_2FO_2 is also zero.⁷² The recommended branching ratio at 298 K for production of CF_3CHFOH in the self-reaction of CF_3CHFO_2 is 0.07, while the study of Nielsen et al.⁷⁵ is consistent with exclusive production of $\text{CHF}_2\text{CF}_2\text{O}$ from the self-reaction of $\text{CHF}_2\text{CF}_2\text{O}_2$. In the chamber experiments, radical–radical reactions such as reaction 11 are artificially emphasized when compared to the real atmosphere. Once again, CH_3O_2 will be the important α -dihydrogenated peroxy radical in the atmosphere.

Again, we have seen that incorporating radical decomposition directly into the Ellis et al.¹⁸ pathway to lower acids leads to yields that are hard to reconcile with the literature. Since radical–radical reactions involving CH_3O_2 likely play an important role in both the mechanisms developed by Ellis et al.,¹⁸ we strongly suggest that additional chamber experiments be performed in which methane is added in varying amounts to the chamber. If Ellis et al.¹⁸ are right, the production of lower PFCAs should rise monotonically with increasing methane mixing ratio. We also echo the concern raised by Tomas et al.⁶¹ about a possible systematic effect caused by using Cl rather than OH radicals as the primary oxidant in the chamber experiments. Generally, using Cl atoms as a faster reacting surrogate for atmospheric OH radicals gives little cause for concern, but in this case, given the modest barriers shown in Table 4, the $\text{C}_n\text{F}_{2n+1}\text{CO}$ radicals formed from the $\text{OH} + \text{C}_n\text{F}_{2n+1}\text{CHO}$ reaction may be strongly predisposed to prompt dissociation, since the reaction enthalpy of $\text{OH} + \text{C}_n\text{F}_{2n+1}\text{CHO}$ is about 16 kcal/mol higher than that of $\text{Cl} + \text{C}_n\text{F}_{2n+1}\text{CHO}$. This effect could further depress the yield of $\text{C}_n\text{F}_{2n+1}\text{C}(\text{O})\text{OH}$. Future PFAL oxidation experiments should be performed with OH rather than Cl radicals wherever possible.

In summary, experimental and theoretical work show that $\text{C}_n\text{F}_{2n+1}\text{CO}$ radicals have a strong tendency to decompose to give $\text{C}_n\text{F}_{2n+1}$ and CO under atmospheric conditions: the lowering of the barrier for decarbonylation of $\text{C}_n\text{F}_{2n+1}\text{CO}$ relative to that of $\text{C}_n\text{H}_{2n+1}\text{CO}$ is well explained by electron withdrawal by F atoms that serve to weaken the critical C–CO bond. Notwithstanding the arguments given by Hurley et al.,⁴¹ the main effect of decarbonylation of $\text{C}_n\text{F}_{2n+1}\text{CO}$ is to decrease the molar yield of $\text{C}_n\text{F}_{2n+1}\text{C}(\text{O})\text{OH}$; if 100% of the $\text{C}_n\text{F}_{2n+1}\text{CO}$ decompose, the yield of $\text{C}_n\text{F}_{2n+1}\text{C}(\text{O})\text{OH}$ must be zero. If the pathway to lower PFCAs proposed by Ellis et al.¹⁸ is correct, there should be a concomitant increase in the yields of $\text{C}_x\text{F}_{2x+1}\text{C}(\text{O})\text{OH}$ for $x < n$. Clearly, there is considerable scope for additional experimental and theoretical studies.

Acknowledgment. We thank Dr. Timothy Wallington (Ford Research), Dr. Gregory Yarwood (ENVIRON International Corporation), Dr. Abdelwahid Mellouki (Laboratoire de Combustion et Systèmes Réactifs, Centre Nationale de la Recherche Scientifique, Orléans), and Professor Howard Sidebottom (University College Dublin) for many helpful discussions.

Supporting Information Available: Computed UMP2/6-31G(d) structures and total energies are provided for the $\text{C}_n\text{F}_{2n+1}\text{CO}$ radicals and the corresponding transition states. This material is available free of charge via the Internet at <http://pubs.acs.org>.

References and Notes

- Calafat, A. M.; Kuklenyik, Z.; Caudill, S. P.; Reidy, J. A.; Needham, L. L. *Environ. Sci. Technol.* **2006**, *40*, 2128.
- Emmett, E. A.; Shofer, F. S.; Zhang, H.; Freeman, D.; Desai, C.; Shaw, L. M. *J. Occup. Environ. Med.* **2006**, *48*, 759.

- (3) Emmett, E. A.; Zhang, H.; Shofer, F. S.; Freeman, D.; Rodway, N. V.; Desai, C.; Shaw, L. M. *J. Occup. Environ. Med.* **2006**, *48*, 771.
- (4) Yeung, L. W. Y.; So, M. K.; Jiang, G.; Taniyasu, S.; Yamashita, N.; Song, M.; Wu, Y.; Li, J.; Giesy, J. P.; Guruge, K. S.; Lam, P. K. S. *Environ. Sci. Technol.* **2006**, *40*, 715.
- (5) Houde, M.; Martin, J. W.; Letcher, R. J.; Solomon, K. R.; Muir, D. C. G. *Environ. Sci. Technol.* **2006**, *40*, 3463.
- (6) Holmström, K. E.; Järnberg, U.; Bignert, A. *Environ. Sci. Technol.* **2005**, *39*, 80.
- (7) Van de Vijver, K. I.; Hoff, P.; Krishna, D.; Brasseur, S.; Van Dongen, W.; Esmans, E.; Reijnders, P.; Blust, R.; De Coen, W. *Environ. Sci. Technol.* **2005**, *39*, 6978.
- (8) Kannan, K.; Corsolini, S.; Falandysz, J.; Fillmann, G.; Kumar, K. S.; Loganathan, B. G.; Mohd, M. A.; Olivero, J.; Van Wouwe, N.; Yang, J. H.; Aldous, K. M. *Environ. Sci. Technol.* **2004**, *38*, 4489.
- (9) Martin, J. W.; Smithwick, M. M.; Braune, B. M.; Hoekstra, P. F.; Muir, D. C. G.; Mabury, S. A. *Environ. Sci. Technol.* **2004**, *38*, 373.
- (10) Martin, J. W.; Whittle, D. M.; Muir, D. C. G.; Mabury, S. A. *Environ. Sci. Technol.* **2004**, *38*, 5379.
- (11) Kannan, K.; Choi, J.-W.; Iseki, N.; Senthilkumar, K.; Kim, D. H.; Masunaga, S.; Giesy, J. P. *Chemosphere* **2002**, *49*, 225.
- (12) Kannan, K.; Newsted, J.; Halbrook, R. S.; Giesy, J. P. *Environ. Sci. Technol.* **2002**, *36*, 2566.
- (13) Giesy, J. P.; Kannan, K. *Environ. Sci. Technol.* **2001**, *35*, 1339.
- (14) Hansen, K. J.; Clemen, L. A.; Ellefson, M. E.; Johnson, H. O. *Environ. Sci. Technol.* **2001**, *35*, 766.
- (15) Giesy, J. P.; Kannan, K. *Environ. Sci. Technol.* **2002**, *36*, 146A.
- (16) Renner, R. *Environ. Sci. Technol.* **2001**, *35*, 154A.
- (17) Ellis, D. A.; Martin, J. W.; Mabury, S. A.; Hurley, M. D.; Andersen, M. P. S.; Wallington, T. J. *Environ. Sci. Technol.* **2003**, *37*, 3816.
- (18) Ellis, D. A.; Martin, J. W.; De Silva, A. O.; Mabury, S. A.; Hurley, M. D.; Andersen, M. P. S.; Wallington, T. J. *Environ. Sci. Technol.* **2004**, *38*, 3316.
- (19) Martin, J. W.; Muir, D. C. G.; Moody, C. A.; Ellis, D. A.; Kwan, W. C.; Solomon, K. R.; Mabury, S. A. *Anal. Chem.* **2002**, *74*, 584.
- (20) Stock, N. L.; Lau, F. K.; Ellis, D. A.; Martin, J. W.; Muir, D. C. G.; Mabury, S. A. *Environ. Sci. Technol.* **2004**, *38*, 991.
- (21) Ellis, D. A.; Martin, J. W.; De Silva, A. O.; Mabury, S. A.; Hurley, M. D.; Andersen, M. P. S.; Wallington, T. J. *J. Phys. Chem. A* **2004**, *108*, 5635.
- (22) Andersen, M. P. S.; Nielsen, O. J.; Toft, A.; Nakayama, T.; Matsumi, Y.; Waterland, R. L.; Buck, R. C.; Hurley, M. D.; Wallington, T. J. *J. Photochem. Photobiol., A* **2005**, *176*, 124.
- (23) D'Eon, J. C.; Hurley, M. D.; Wallington, T. J.; Mabury, S. A. *Environ. Sci. Technol.* **2006**, *40*, 1862.
- (24) Goss, K.-U.; Bronner, G.; Harner, T.; Hertel, M.; Schmidt, T. C. *Environ. Sci. Technol.* **2006**, *40*, 3572.
- (25) Krusic, P. J.; Marchione, A. A.; Davidson, F.; Kaiser, M. A.; Kao, C.-P. C.; Richardson, R. E.; Botelho, M.; Waterland, R. L.; Buck, R. C. *J. Phys. Chem. A* **2005**, *109*, 6232.
- (26) Stock, N. L.; Ellis, D. A.; Deleebeek, L.; Muir, D. C. G.; Mabury, S. A. *Environ. Sci. Technol.* **2004**, *38*, 1693.
- (27) Arp, H. P. H.; Niederer, C.; Goss, K.-U. *Environ. Sci. Technol.* **2006**, *40*, 7298.
- (28) Goss, K.-U.; Bronner, G. *J. Phys. Chem. A* **2006**, *110*, 9518.
- (29) Wallington, T. J.; Hurley, M. D.; Xia, J.; Wuebbles, D. J.; Sillman, S.; Ito, A.; Penner, J. E.; Ellis, D. A.; Martin, J. W.; Mabury, S. A.; Nielsen, O. J.; Andersen, M. P. S. *Environ. Sci. Technol.* **2006**, *40*, 924.
- (30) Yarwood, G.; Kemball-Cook, S.; Keinath, M.; Washburn, S.; Waterland, R. L.; Buck, R. C.; Korzenowski, S. H.; Russell, M. H. High resolution atmospheric modeling of fluorotelomer alcohols and perfluorocarboxylic acids in the North American troposphere. Presented at Dioxin 2006, Oslo, 2006.
- (31) Arctic Monitoring and Assessment Programme (AMAP). *AMAP Assessment 2002: Persistent Organic Pollutants in the Arctic*; Oslo, Norway, 2004. Also available in electronic form from the AMAP Web site: <http://www.amap.no>.
- (32) Li, Y.-F.; Macdonald, R. W.; Jantunen, L. M. M.; Harner, T.; Bidleman, T. F.; Strachan, W. M. J. *Sci. Total Environ.* **2002**, *291*, 229.
- (33) Kelly, T.; Bossoutrot, V.; Magneron, I.; Wirtz, K.; Treacy, J.; Mellouki, A.; Sidebottom, H.; Le Bras, G. *J. Phys. Chem. A* **2005**, *109*, 347.
- (34) Vésine, E.; Bossoutrot, V.; Mellouki, A.; Le Bras, G.; Wenger, J.; Sidebottom, H. *J. Phys. Chem. A* **2000**, *104*, 8512.
- (35) Andersen, M. P. S.; Nielsen, O. J.; Hurley, M. D.; Ball, J. C.; Wallington, T. J.; Ellis, D. A.; Martin, J. W.; Mabury, S. A. *J. Phys. Chem. A* **2005**, *109*, 1849.
- (36) Sellevåg, S. R.; Kelly, T.; Sidebottom, H.; Nielsen, C. J. *Phys. Chem. Chem. Phys.* **2004**, *6*, 1243.
- (37) Andersen, M. P. S.; Nielsen, O. J.; Hurley, M. D.; Ball, J. C.; Wallington, T. J.; Stevens, J. E.; Martin, J. W.; Ellis, D. A.; Mabury, S. A. *J. Phys. Chem. A* **2004**, *108*, 5189.
- (38) Nakayama, T.; Takahashi, K.; Matsumi, Y.; Toft, A.; Andersen, M. P. S.; Nielsen, O. J.; Waterland, R. L.; Buck, R. C.; Hurley, M. D.; Wallington, T. J. *J. Phys. Chem. A* **2007**, *111*, 909.
- (39) Chiaperro, M. S.; Malanca, F. E.; Argüello, G. A.; Wooldridge, S. T.; Hurley, M. D.; Ball, J. C.; Wallington, T. J.; Waterland, R. L.; Buck, R. C. *J. Phys. Chem. A* **2006**, *110*, 11944.
- (40) Solignac, G.; Mellouki, A.; Le Bras, G.; Barnes, I.; Benter, T. J. *J. Phys. Chem. A* **2006**, *110*, 4450.
- (41) Hurley, M. D.; Ball, J. C.; Wallington, T. J.; Andersen, M. P. S.; Nielsen, O. J.; Ellis, D. A.; Martin, J. W.; Mabury, S. A. *J. Phys. Chem. A* **2006**, *110*, 12443.
- (42) Jagiella, S.; Libuda, H. G.; Zabel, F. *Phys. Chem. Chem. Phys.* **2000**, *2*, 1175.
- (43) Frisch, M. J.; Trucks, G. W.; Schlegel, H. B.; Scuseria, G. E.; Robb, M. A.; Cheeseman, J. R.; Montgomery, J. A., Jr.; Vreven, T.; Kudin, K. N.; Burant, J. C.; Millam, J. M.; Iyengar, S. S.; Tomasi, J.; Barone, V.; Mennucci, B.; Cossi, M.; Scalmani, G.; Rega, N.; Petersson, G. A.; Nakatsuji, H.; Hada, M.; Ehara, M.; Toyota, K.; Fukuda, R.; Hasegawa, J.; Ishida, M.; Nakajima, T.; Honda, Y.; Kitao, O.; Nakai, H.; Klene, M.; Li, X.; Knox, J. E.; Hratchian, H. P.; Cross, J. B.; Adamo, C.; Jaramillo, J.; Gomperts, R.; Stratmann, R. E.; Yazyev, O.; Austin, A. J.; Cammi, R.; Pomelli, C.; Ochterski, J. W.; Ayala, P. Y.; Morokuma, K.; Voth, G. A.; Salvador, P.; Dannenberg, J. J.; Zakrzewski, V. G.; Dapprich, S.; Daniels, A. D.; Strain, M. C.; Farkas, O.; Malick, D. K.; Rabuck, A. D.; Raghavachari, K.; Foresman, J. B.; Ortiz, J. V.; Cui, Q.; Baboul, A. G.; Clifford, S.; Cioslowski, J.; Stefanov, B. B.; Liu, G.; Liashenko, A.; Piskorz, P.; Komaromi, I.; Martin, R. L.; Fox, D. J.; Keith, T.; Al-Laham, M. A.; Peng, C. Y.; Nanayakkara, A.; Challacombe, M.; Gill, P. M. W.; Johnson, B.; Chen, W.; Wong, M. W.; Gonzalez, C.; Pople, J. A. *Gaussian 03*, revision B.05; Gaussian, Inc.: Wallingford, CT, 2003.
- (44) Dennington, R., II; Keith, T.; Millam, J.; Eppinnett, K.; Hovell, W. L.; Gilliland, R. *GaussView*, revision 3.09; Semichem, Inc.: Shawnee Mission, KS, 2003.
- (45) Möller, C.; Plesset, M. S. *Phys. Rev.* **1934**, *46*, 618.
- (46) Bartlett, R. J. *Annu. Rev. Phys. Chem.* **1981**, *32*, 339.
- (47) Franci, M. M.; Pietro, W. J.; Hehre, W. J.; Binkley, J. S.; Gordon, M. S.; DeFrees, D. J.; Pople, J. A. *J. Chem. Phys.* **1982**, *77*, 3654.
- (48) Scott, A. P.; Radom, L. *J. Phys. Chem.* **1996**, *100*, 16502.
- (49) Dixon, D. A.; Fukunaga, T.; Smart, B. E. *J. Am. Chem. Soc.* **1986**, *108*, 1585.
- (50) Lentz, D.; Bach, A.; Buschmann, J.; Luger, P.; Messerschmidt, M. *Chem.—Eur. J.* **2004**, *10*, 5059.
- (51) Baker, J.; Muir, M. J. *Fluorine Chem.* **1998**, *89*, 145.
- (52) Krishnan, R.; Frisch, M. J.; Pople, J. A. *J. Chem. Phys.* **1980**, *72*, 4244.
- (53) Krishnan, R.; Binkley, J. S.; Seeger, R.; Pople, J. A. *J. Chem. Phys.* **1980**, *72*, 650.
- (54) Francisco, J. S.; Abersold, N. J. *J. Chem. Phys. Lett.* **1991**, *187*, 354.
- (55) Francisco, J. S. *J. Chem. Phys. Lett.* **1992**, *191*, 7.
- (56) Maricq, M. M.; Szente, J. J.; Khitrov, G. A.; Dibble, T. S.; Francisco, J. S. *J. Phys. Chem.* **1995**, *99*, 11875.
- (57) Viskolcz, B.; Bérces, T. *Phys. Chem. Chem. Phys.* **2002**, *2*, 5430.
- (58) Wolinski, K.; Pulay, P. *J. Chem. Phys.* **1989**, *90*, 3647.
- (59) Watkins, K. W.; Word, W. W. *Int. J. Chem. Kinet.* **1974**, *6*, 855.
- (60) Watkins, K. W.; Thompson, W. W. *Int. J. Chem. Kinet.* **1973**, *5*, 791.
- (61) Tomas, A.; Caralp, F.; Lesclaux, R. Z. *Phys. Chem. (Munich)* **2000**, *214*, 1349.
- (62) O'Neal, E.; Benson, S. W. *J. Chem. Phys.* **1962**, *36*, 2196.
- (63) Barnes, I.; Becker, K. H.; Kirchner, F.; Zabel, F.; Richer, H.; Sodeau, J. Formation and thermal decomposition of $CCl_3C(O)O_2NO_2$ and $CF_3C(O)O_2NO_2$. Presented at the Step-Halocside/AFEAS Workshop, March 1993, Dublin.
- (64) Méreau, R.; Rayez, M.-T.; Rayez, J.-C.; Caralp, F.; Lesclaux, R. *Phys. Chem. Chem. Phys.* **2001**, *3*, 4712.
- (65) Hehre, W. J.; Radom, L.; Schleyer, P. v. R.; Pople, J. A. *Ab Initio Molecular Orbital Theory*; John Wiley & Sons: New York, 1986.
- (66) Glendening, E. D.; Reed, A. E.; Carpenter, J. E.; Weinhold, F. NBO, version 3.1.
- (67) Mack, H.-G.; Steger, B.; Oberhammer, H. *Chem. Phys. Lett.* **1986**, *129*, 582.
- (68) Andersen, M. P. S.; Stenby, C.; Nielsen, O. J.; Hurley, M. D.; Ball, J. C.; Wallington, T. J.; Martin, J. W.; Ellis, D. A.; Mabury, S. A. *J. Phys. Chem. A* **2004**, *108*, 6325.
- (69) Hasson, A. S.; Tyndall, G. S.; Orlando, J. J. *J. Phys. Chem. A* **2004**, *108*, 5979.
- (70) Andersen, M. P. S.; Hurley, M. D.; Wallington, T. J.; Ball, J. C.; Martin, J. W.; Ellis, D. A.; Mabury, S. A. *J. Phys. Chem. Lett.* **2003**, *381*, 14.
- (71) Andersen, M. P. S.; Hurley, M. D.; Wallington, T. J.; Ball, J. C.; Martin, J. W.; Ellis, D. A.; Mabury, S. A.; Nielsen, O. J. *J. Phys. Chem. Lett.* **2003**, *379*, 28.
- (72) Atkinson, R.; Baulch, D. L.; Cox, R. A.; Crowley, J. N.; Hampson, R. F. J.; Hynes, R. G.; Jenkin, M. E.; Kerr, J. A.; Rossi, M. J.; Troe, J.

Summary of Evaluated Kinetic and Photochemical Data for Atmospheric Chemistry; IUPAC Subcommittee on Gas Kinetic Data Evaluation for Atmospheric Chemistry, 2006.

(73) Tuazon, E. C.; Atkinson, R. *Environ. Sci. Technol.* **1994**, 28, 2306.

(74) Nielsen, O. J.; Ellermann, T.; Bartkiewicz, E.; Wallington, T. J.; Hurley, M. D. *Chem. Phys. Lett.* **1992**, 192, 82.

(75) Nielsen, O. J.; Ellermann, T.; Sehested, J.; Wallington, T. J. *J. Phys. Chem.* **1992**, 96, 10875.